Size-dependent plasticity in contact/friction: from discrete dislocation dynamics inside an asperity to statistical summation over asperities

Song, Hengxu

2

Statistical Model of Asperity Interaction In Rough Surfaces Contact

Asperities on a rough surface are not isolated, but connected through the substrate. Therefore, for a rough surface in contact, deformation of a contacting asperity will also shift its neighboring asperities down through substrate deformation, i.e., interaction deformation. The magnitude of the interaction depends on the distance to the contacting asperity. In this chapter, we present a method to account for asperity interaction through the statistical summation of asperities forces. Asperity interaction is found to reduce the contact force compared with the contact force if the asperities would deform independently. We also investigate the dependence of interaction effect on material properties as well as surface roughness. After extending the model for a finite surface area assumption, the model is found to be consistent with other existed models for a finite surface area.

The Chapter is an extended version of Song, H., van der Giessen, E. and Vakis, A.I., 2016, Erratum: "Asperity Interaction and Substrate Deformation in Statistical Summation Models of Contact Between Rough Surfaces" [J. Appl. Mech., 81(4), 041012. Author: Vakis, A.I.], J. Appl. Mech., **83**(8):087001-087001-1.

2.1. Introduction

Understanding the contact between surfaces at small size scales is very important to many engineering applications, such as microelectromechanical systems (MEMS) and hard-disk drivers. Asperities result in the actual contact of a rough surface being a small fraction of the nominal surface area. The rough surface contact problem is actually the study of the collective behaviors of contacting asperities on the surface. The model by Greenwood and Williamson (GW) [1] forms the basis of many subsequent works [2, 3, 4, 5, 6, 7] on rough surface contact. In the original GW model, asperities with spherical tips deform independently. However, asperities on the surface have a common substrate through which they are connected. Thus, pressing one asperity will shift all its neighbors down; this is called the asperity interaction effect. The interaction effect is naturally included in finite element (FE) models of bodies in contact [8, 9], but these models suffer from computational costs. Ciavarella *et al.* [7] extended the GW model to incorporate the asperity interaction effect for a finite surface area. In their model, asperity interaction is implemented by shifting the substrate; the amount of shifting utilizes the analytical solution of the deformation caused by a uniform pressure distributed over the surface with finite size. The interaction effect is seen to decrease the contact force. However, in [7], the asperities are assumed to deform elastically, while it is well known that asperities can deform plastically, even at small contact loads.

Through FEM, Kogut and Etsion [5] (KE) numerically studied the contact between a sphere and a rigid flat. The contact force was parameterized as a function of the sphere interference which accounts for elastic, elasto-plastic and fully plastic regimes. Following a different route to implement asperity interaction than Ciavarella *et al.* [7], Vakis [12] proposed a statistical model for elasto-plastic (KE type) asperity contact. In the model, the interaction effect was considered only for non-contacting asperities that have taller contacting neighbors. However, interaction effect also exists for contacting asperities once they have neighboring asperities in contact.

In this chapter, we extend the model proposed by Vakis [12] to include the interaction effect based on the probability of having asperities in contact, regardless of whether the neighbors are taller or not. Following the GW model [1], the roughness of two contacting surfaces is combined into one rough surface that comes into contact with a rigid flat, shown in Fig. 2.1. It is assumed that the topography of the rough surface can be described as a collection of asperities with radius curvature of R that are distributed in the surface plane with density η and a normal

(Gaussian) distribution of their heights with standard deviation σ_s.

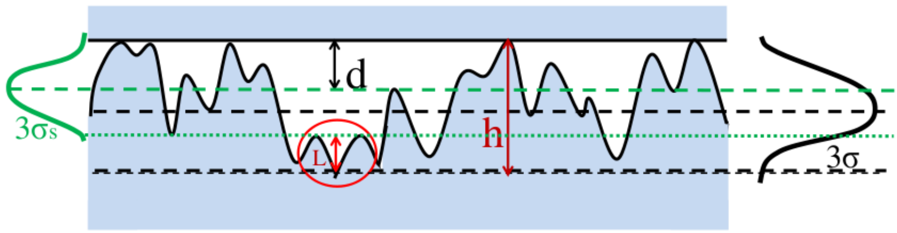

Figure 2.1: Schematic representation of the stochastic rough surface contact problem: both the asperity height and the surface height follow a Gaussian distribution with standard deviation σ_s and σ, respectively. Asperity height h is measured from the substrate where material is continuous. The distance between the surface mean height and the rigid flat is d.

Contacting asperities are considered to effectively reduce the height of their neighbors, so that the asperity mean height of the whole surface becomes smaller. Following [7, 10], the simplifying assumption is made that the asperity interaction effect can be adequately captured by modifying the asperity height distribution as a function of the mean plane separation. Strictly speaking, the change of the height distribution should include two aspects: asperity average height and standard deviation σ_s. However, since a statistical model does not deal with any single asperity, the evolution of σ_s is unknown. Therefore it is assumed that σ_s does not evolve with the mean plane separation, and the asperity interaction effect is reflected just by an equivalent shift of the asperity mean height.

2.2. A probabilistic model of asperity interaction

The surface height statistics, determined from an experimentally obtained surface profile, can be fitted to a Gaussian distribution with standard deviation of σ. The asperity height distribution is different from the surface height distribution as the former does not contain the information of valleys. The standard deviation of the asperity height distribution σ_s is connected to that of the surface height distribution σ according to [3]:

$$\sigma_s = \sqrt{\sigma^2 - \frac{3.717 \times 10^{-4}}{\eta^2 R^2}},$$

where R is asperity mean radius and η is the asperity density. For a normal distribution, an envelop of $\pm 3\sigma$ around the surface mean plane includes 99.7% of the surface height distribution, so we define the initial position of the rigid flat to be 3σ, i.e., the initial mean plane separation $d = 3\sigma$. With increasing load, d decreases from 3σ to 0, at the moment that the surface mean is reached.

We nondimensionalize the asperity height z and the mean plane separation d $z^* = z/\sigma$ and $d^* = d/\sigma$. The probability density function of the normalized asperity height then becomes

$$\varphi^*(z^*) = \frac{1}{\sqrt{2\pi}}\left(\frac{\sigma}{\sigma_s}\right)\exp\left[-\frac{1}{2}\left(\frac{\sigma}{\sigma_s}\right)^2(z^*)^2\right].$$

Thus, the probability that asperities are in contact–i.e., taller than the mean plane separation– is

$$\text{prob}(z^* > d^*) = \int_{d^*}^{\infty}\varphi^*(z^*)\mathrm{d}z^*.$$

Assuming asperities are uniformly distributed in an infinite plane, given a single

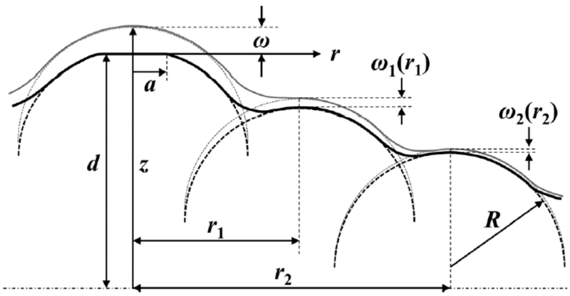

Figure 2.2: Schematic representation of asperity interaction: a contacting asperity (local interference ω) shifts down its two neighbors by the magnitudes of $\omega_1(r_1)$, $\omega_2(r_2)$ respectively.

contacting asperity, shown in Fig. 2.2, the distance from n^{th} neighbor asperity to the contacting asperity r_n is defined as [11]

$$r_n = \frac{1}{\sqrt{\pi}}\frac{\Gamma(n+\frac{1}{2})}{\Gamma(n)}\frac{1}{\sqrt{\eta}}, \tag{2.1}$$

where Γ is the Gamma function.

As the contacting asperity is pressed downwards by a displacement ω, all neighbor asperities will be shifted down due to asperity interactions. The shift of n^{th} neighbor asperity $\omega_n = f(\omega, r_n)$ (to be explained in detail in the next section) depends on the local interference of the contacting asperity ω ($\omega = z - d$) and the distance to the contacting asperity r_n, as illustrated in Fig. 2.2. The total number of n^{th} neighbors is $k_n = \eta\pi(r_n^2 - r_{n-1}^2)$, thus the total amount of shift caused by a contacting asperity is:

$$\Omega_a = \sum_{i=1}^{n} \omega_i k_i = \eta \{\pi r_1^2 f(z,r_1) + \pi(r_2^2 - r_1^2) f(z,r_2) + \pi(r_3^2 - r_2^2) f(z,r_3) + \dots + \pi(r_n^2 - r_{n-1}^2) f(z,r_n)\}. \tag{2.2}$$

Averaging Ω_a by the total number of all asperities on the surface N gives the effective shift of the mean asperity heights caused by one contacting asperity. Therefore, for the whole surface, all contacting asperities cause the effective shift (in dimensionless form) to be:

$$\Omega^*(d^*) = \frac{N\int_{d^*}^{\infty} \Omega_a^* \varphi^*(z^*)\mathrm{d}z^*}{N} = \int_{d^*}^{\infty} \Omega_a^* \varphi^*(z^*)\mathrm{d}z^*, \tag{2.3}$$

where $\Omega_a^* = \Omega_a/\sigma$. Unlike the formulations in [12] where the interaction effect was considered only for non-contacting asperities, the above formulation considers asperity interaction from the contacting asperities and sequentially calculates the substrate deformation of its neighbors. Thus, a contacting asperity can also feel the interaction effect from other contacting asperities.

2.3. The mechanics of multiasperity contact

Asperity interaction effect is achieved through the substrate. Like in [10], we define the substrate to be the base of the shortest asperity such that continuity of the substrate is guaranteed. Moreover, the substrate is assumed to be the point of intersection of the two lowest asperities with the equal height, In [12], the profile of asperities is assumed to obey a parabolic form with radius of curvature of R at the asperity tip, shown in red circle in Fig. 2.1. The point of intersection between two parabolas whose vertices are shifted along the radial direction by a distance r_1 (as they are the closest neighbor) is located at $L = r_1^2/8R$ below their vertices. Accounting for the lower limit of the roughness envelope (at three standard deviations below the mean), the distance between the rigid flat and substrate, as illustrated in Fig. 2.1, is

$$h = \left(\frac{r_1^2}{8R} + 3\sigma_s\right) + d = \left(\frac{1}{32R\eta} + 3\sigma_s\right) + d.$$

When a asperity comes into contact with the rigid flat, the maximum Hertz pressure p_0 at the asperity contact interface is

$$p_0 = \frac{2E}{\pi}\sqrt{\frac{\sigma}{R}(z^* - d^*)},$$

and the contact patch radius is

$$a = \frac{\pi p_0 R}{2E} = \sqrt{\sigma R(z^* - d^*)}.$$

Following [10], we assume the traction profile at the substrate level has the same shape with the Hertz distribution at the contact interface, but with a different magnitude. The maximum contact pressure decreases from the contact interface

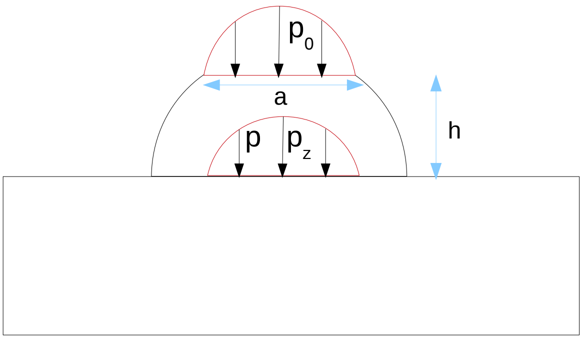

Figure 2.3: Schematic of the pressure profile. The shape of the pressure profile on the substrate is assumed to be the same with it on the contact surface, but with a different magnitude.

to the substrate with the square of the distance h (shown in Fig. 2.3) in between:

$$p_z = p_0\left[1 + \left(\frac{h}{a}\right)^2\right]^{-1}.$$

Though the assumption violates force equilibrium for each asperity, the verification by FEM [10] shows the validity when the asperity spacing is small. Thus, the normal pressure applied at the substrate level is calculated as

$$p = p_z\left(1 - \left(\frac{r}{a}\right)^2\right)^{1/2},$$

where r is the distance to the center of the contact. The normal pressure at the substrate under the contacting asperity gives the normal displacement as a function of the radial distance from the center of the contact according to the Hertz solution as [13]

$$u_z(r) = \begin{cases} \dfrac{1-\nu^2}{E}\dfrac{p_z}{2a}\left[(2a^2-r^2)\sin^{-1}\left(\dfrac{a}{r}\right)+r^2\left(\dfrac{a}{r}\right)\left(1-\dfrac{a^2}{r^2}\right)^{1/2}\right] & \text{for } r > a \\ \dfrac{1}{R}\left(a^2-\dfrac{r^2}{2}\right) & \text{for } r \le a \end{cases} \tag{2.4}$$

where ν is Poisson's ratio. We can see in above equations that the actual amount of the shift for n^{th} neighbor asperity $\omega_n = f(\omega, r_n)$ depends on the local interference of the contacting asperity ω ($\omega = h - d$) which determines the normal pressure on the substrate and the distance to the contacting asperity r_n which influence the normal displacement. The effect of the lateral displacement $u_r(r)$ on the spacing between asperities is not taken into account. As each contacting asperity tends to 'pull' its neighbors closer, for the whole surface, the effect is neutralized.

For a contacting asperity, the dimensionless load as a function of interference is adopted from the Kogut-Etsion (KE) model of contact between a sphere and a rigid flat [4, 5]. Different regimes during the contact (elastic, elasto-plastic, and fully plastic) are parametrized as follows:

$$\frac{P}{P_c} = \begin{cases} \omega^{*1.5} & \text{for } \omega^* \le 1 \\ 1.03\omega^{*1.425} & \text{for } 1 < \omega^* \le 6 \\ 1.4\omega^{*1.263} & \text{for } 6 < \omega^* \le 110 \\ \dfrac{3}{K}\omega^* & \text{for } \omega^* > 110 \end{cases}$$

where $\omega^* = \omega/\omega_c$ is the dimensionless interference, $\omega_c = \left(\dfrac{\pi K H}{2E^*}\right)^2 R = \omega_c^*\sigma$ is the critical interference when plasticity happens. $P_c = \dfrac{2}{3}KH\pi\omega R$ is the load related at the onset of the plasticity. Material hardness $H = 2.8\sigma_Y$ and factor $K = 0.454 + 0.4\nu$.

Based on the mechanical response of a single asperity described above, the total dimensionless contact force of a rough surface can be calculated as [5]:

$$P^* = \frac{P}{A_n H} = \frac{2}{3}\pi\beta K\omega_c^* \left[\int_{d^*}^{d^*+\omega_c^*} I^{1.5}\varphi^*(z^*)dz^* + 1.03 \int_{d^*+\omega_c^*}^{d^*+6\omega_c^*} I^{1.425}\varphi^*(z^*)dz^* + \right.$$
$$\left. 1.4 \int_{d^*+6\omega_c^*}^{d^*+110\omega_c^*} I^{1.263}\varphi^*(z^*)dz^* + \frac{3}{K}\int_{d^*+110\omega_c^*}^{\infty} I\varphi^*(z^*)dz^* \right], \quad (2.5)$$

where the integrand is

$$I = \left(\frac{z^* - d^*}{\omega_c^*}\right)$$

for local asperity interference $\omega = z - d$. The prefactor β is defined as $\beta = \sigma R\eta$.

When asperity interaction is absent, asperity height distribution $\varphi^*(z^*)$ does not vary under contact. However, when we take into account asperity interaction, the effective shift down of the mean of asperity heights $\Omega^*(d^*)$ defined in Eq.(2.3) changes the asperity height distribution into

$$\varphi^*(z^* = \frac{1}{\sqrt{2\pi}}\left(\frac{\sigma}{\sigma_s}\right)\exp\left[-\frac{1}{2}\left(\frac{\sigma}{\sigma_s}\right)^2 (z^* + \Omega^*(d^*))^2\right].$$

Moreover, it evolves with the loading.

2.4. The effect of the order of interaction

Since the asperity interaction is calculated via the Hertz solution which decays as a function of distance from the contact, one would expect that the effect of interaction becomes negligible far away from the contacting asperity. However, this was not the case in [12] where the effect grew unboundedly, as pointed out in the recent erratum [14]. Figure 2.4 shows the cumulative dimensionless interaction deformation Ω^* defined in Eq.(2.3) as a function of the dimensionless mean plane separation d^* (decreasing d^* means increasing loading) for various values of n. It can be seen that Ω^* converges when the order of interaction is large enough. It can also be seen that convergence becomes difficult with decreasing d^*. The reason is that Ω^* also depends on the loading: the larger load leads to a higher stress on the substrate, and the normal displacement caused by the higher stress decays to zero far away from the contact.

The dimensionless contact force P^* as a function of d^* is plotted in Fig. 2.5(a). Compared with the nominal model [5] where asperities are assumed to deform independently, asperity interaction delays the onset of contact, and thus yields a smaller contact force at a given separation. As the interaction effect converges

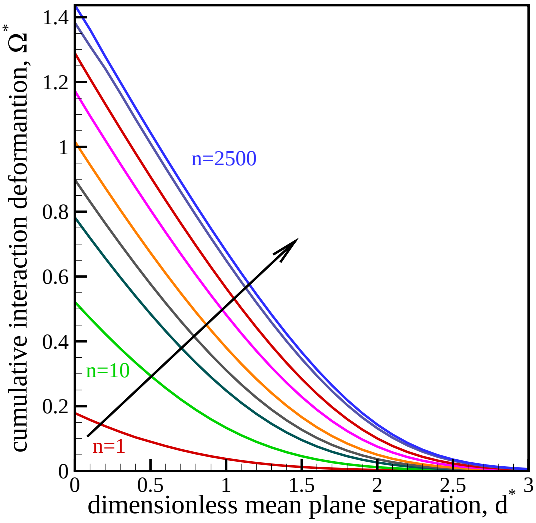

Figure 2.4: Dimensionless cumulative interaction versus mean plane separation for increasing order of interactions.

with increasing n (shown in Fig. 2.4), P^* is expected to converge as well. This can be seen in Fig. 2.5(b): the value of P^* at mean plane separation $d^* = 0$ clearly starts to converge when the order of interaction is $n \geq 1000$.

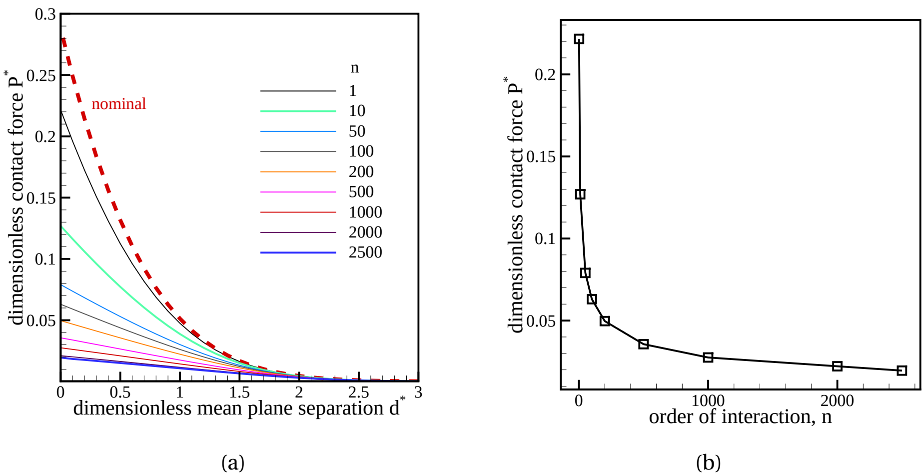

Figure 2.5: (a) Dimensionless contact force versus mean plane separation for various orders of interactions, (b) dimensionless contact force at $d^* = 0$ for various orders of interactions.

2.5. Influence of roughness and material properties

The dependence of the interaction effect on the roughness parameters R, σ, η is shown in Fig. 2.6. The asperity radius R and the height of contacting asperities enter interaction effect through the Hertzian solution for individual asperities. Fig. 2.6(a) and Fig. 2.6(b) show that the asperity interaction effect increases with increasing R and σ. The asperity density η influences the total number of n^{th} order neighbors, and Fig. 2.6(c) shows that increasing η results in a stronger interaction effect. Contrary to the findings in [12], different combinations of R, σ, η, for the same $\beta = R\sigma\eta$, do not yield identical results (shown by the thick black lines for the case of $\beta = 1$). Therefore even though β appears as a pre-factor in the expression of P^* in Eq. (5.10), it is not the single governing parameter that controls the interaction effect. Actually, Buckingham Π theorem indicates that the dimensionless contact force as a function of three roughness parameters R, σ, η should depend on two dimensionless groups. β is one dimensionless parameter, if we use R/σ as the other dimensionless parameter, then different combinations of roughness parameters that have the same β and R/σ should yield identical result. This is shown in Fig. 2.7(a) where two groups of roughness parameters have: $\beta = 1, R/\sigma = 50$.

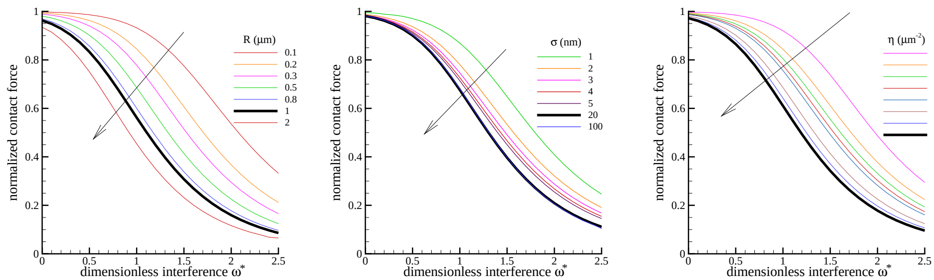

Figure 2.6: Normalized contact force P^*/P^{nom} versus dimensionless interference ($\omega^* = 3 - d^*$) for various roughness parameters, (a) R (with $\sigma = 10\text{nm}$, $\eta = 100/\mu\text{m}^2$), (b) σ (with $R = 0.5\mu\text{m}$, $\eta = 100/\mu\text{m}^2$), (c) η (with $R = 0.5\mu\text{m}$, $\sigma = 10\text{nm}$). Arrows indicate the increase of value of the parameter.

A 3^2 full factorial study was conducted for the variable material properties summarized in Table 2.1. No dependence on material properties was found as shown in Fig. 2.7(b).

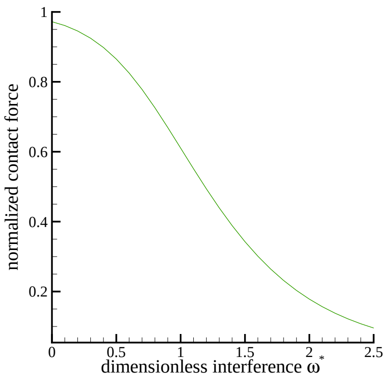

(a)

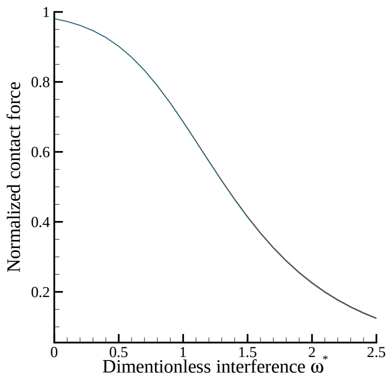

(b)

Figure 2.7: Normalized contact force P^*/P^{nom} versus dimensionless interference ($\omega^* = 3 - d^*$), (a) for two groups of roughness parameters $\sigma = 10$nm, R= 0.5μm, $\eta = 200\mu\text{m}^{-2}$ and $\sigma = 14.1$nm, R= 0.707μm, $\eta = 100\mu\text{m}^{-2}$, (b) for different material properties ($\sigma = 10$nm, R= 0.5μm, and $\eta = 100\mu\text{m}^{-2}$).

Table 2.1: Material properties for factorial study

Reduced mod., E^* (GPa)	50	70	90
Hardness, H (GPa)	5.29	10.29	15.29
Poisson ratio, ν	0.2	0.3	0.4

2.6. Comparison with models based on a finite surface area A

Ciavarella *et al.* [7] incorporated asperity interaction through deformation of the substrate caused by a uniform pressure distributed over, and restricted to, a finite surface area A. In the statistical model, for a finite A, the n^{th} order interaction distance becomes $r_n = n/\sqrt{\eta}$ (Eq. (2.1) is only valid for an infinite large A), with $1/\sqrt{\eta}$ representing the average asperity spacing.

Fig. 2.8 shows a comparison, for different values of surface area A, between the predictions of our model and the model in which asperity interaction is implemented through the method of Ciavarella *et al* [7]. Interestingly, the two predictions match exactly when we use the maximum physically meaningful order of interaction $n_{\max} = \sqrt{A\eta} - 1$. Furthermore, the interaction effect for a larger area

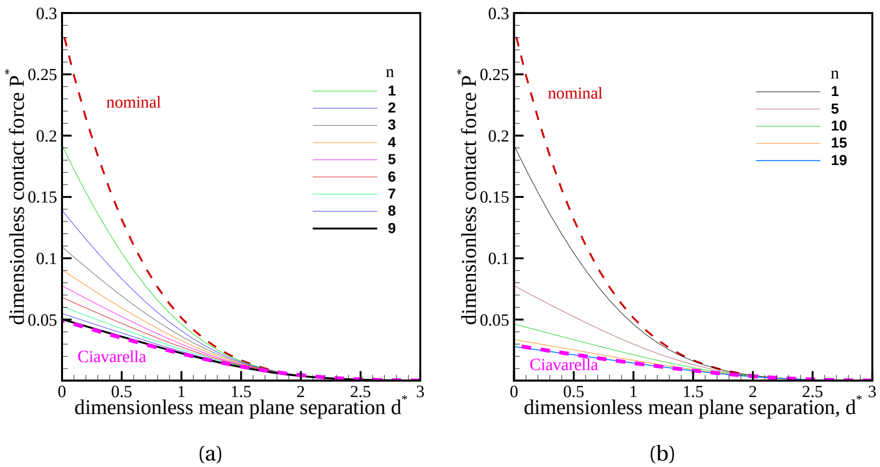

Figure 2.8: Comparison with Ciavarella's model for various orders of interactions when asperity density $\eta = 100/\mu\text{m}^2$. (a) When nominal area $A = 1\mu\text{m}^2$ ($n_{\text{max}} = \sqrt{A\eta} - 1 = 9$), (b) $A = 4\mu\text{m}^2$ ($n_{\text{max}} = \sqrt{A\eta} - 1 = 19$).

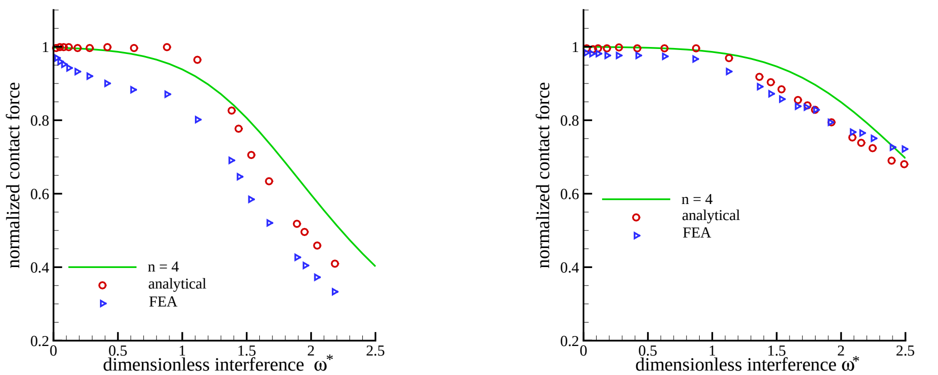

Figure 2.9: Comparison of normalized (by nominal force) contact force P^*/P^{nom} versus dimensionless interference ($\omega^* = 3 - d^*$) with Chandrasekar's analytical and FEA predictions for different values of asperity spacing $d = 1/\sqrt{\eta}$: (a) $0.2R$, (b) $0.7R$.

($A = 4\mu\text{m}^2$ in Fig. 2.8 (b)) is stronger than it is for a smaller A ($= 1\mu\text{m}^2$ in Fig. 2.8 (a)). This means that the interaction effect increases with increasing A if one assumes a finite surface area. This effect is unlimited, i.e., there is no convergence in the statistical model when using $r_n = n/\sqrt{\eta}$. This emphasizes that the interaction effect relies on the convergence of $\Omega_{a,n} = \eta\pi(r_n^2 - r_{n-1}^2)f(z, r_n)$ in Eq. (2.2) to zero for large n. For an infinitely large surface, the latter convergence is guaranteed by the statistical description of r_n given in Eq. (2.1); it is not the case if we restrict the interaction model to a finite area of size A with $r_n = n/\sqrt{\eta}$.

The model for finite A is also compared to the FEA and analytical models of Chandrasekar *et al.* [10], even though they consider a number of asperities (25) asperities that is too small to be statistically significant. Nevertheless, good agreement is found, as shown in Fig. 2.9, for asperity interaction orders of $\sqrt{25} - 1 = 4$.

2.7. Summary and Conclusions

Asperity interaction has been studied in the present chapter within the context of statistical summation models of rough surface contact, based on the probability that contacting asperities shift down their neighbors through substrate deformation. The mechanical response of the asperity is characterized by Kogut and Etsion's finite element solutions for elastic, elasto-plastic, and fully plastic normal contact. The maximum normal pressure acting on the substrate is scaled from the maximum Hertzian pressure with the square of the depth, and the substrate deformation is calculated from the Hertz solution in a half space.

The salient conclusions of this study are:

1. The model for an infinite large surface area A shows convergence of the interaction effect.

2. The asperity interaction effect depends on the individual characteristics, R, σ, η. Normalized contact force depends on two dimensionless parameters β and R/σ. No dependence was found on material properties.

3. The model based on a finite surface area of size A is found to be consistent with models based on a finite surface area assumption.

Validation of our statistical model requires a discrete asperity model. The discrete asperity model can also provide the evolution of σ_s, which may subsequently be implemented in the statistical model to provide a more accurate interaction effect.

References

[1] J.A. Greenwood, J.B.P. Williamson, 1966. Contact of nominally flat surfaces, Proc. R. Soc. Lond. A., **295**(1442), 300-319.

[2] A.W. Bush, R.D. Gibson, T.R. Thomas, 1975. The elastic contact of a rough surface, Wear, **35**(1), 87-111.

[3] J.I. McCool, 1986. Comparison of models for the contact of rough surfaces, Wear, **107**(1), 37-60.

[4] W.R. Chang, I. Etsion, D.B. Bogy, 1987. An elastic-plastic model for the contact of rough surfaces, ASME J. Tribol., **109**(2), 257-263.

[5] L. Kogut, I. Etsion, 2002. Elastic-plastic contact analysis of a sphere and a rigid flat, J. Appl. Mech., **69**(5), 657-662.

[6] M. Ciavarella, V. Delfine, G. Demelio, 2006. A re-vitalized Greenwood and Williamson model of elastic contact between fractal surfaces, J. Mech. Phys. Solids, **54**(12), 2569-2591.

[7] M. Ciavarella, J. A. Greenwood, M. Paggi, 2008. ”Inclusion of ”interaction” in the Greenwood and Williamson contact theory,” Wear, vol. 265, 729-734.

[8] K. Komvopoulos, N. Ye, 2001. Three-dimensional contact analysis of interacting asperities in contact with a rigid flat,” ASME J. Tribol., **123**(3), 632-640.

[9] H. Eid, G.G. Adams, 2007. An elastic-plastic finite element analysis of interacting asperities in contact with a rigid flat,” J. Phys. D Appl. Phys., **123**(3), 7432-7439.

[10] S. Chandrasekar, M. Eriten and A. A. Polycarpou, 2013. An Improved Model of Asperity Interaction in Normal Contact of Rough Surfaces, J. Appl. Mech., vol. 80, 011025.

[11] P. Bhattacharyya, B.K. Chakrabarti, 2008. The mean distance to the nth neighbour in a uniform distribution of random points: an application of probability theory, Eur. J. Phus., **29**(3), 639.

[12] A. I. Vakis, 2014. Asperity Interaction and Substrate Deformation in Statistical Summation Models of Contact Between Rough Surfaces, J. Appl. Mech., 81(4), 41012.

[13] K.L. Johnson, 1985, *Contact Mechanics*, Cambridge University Press, Cambridge, UK.

[14] H. Song, E. van der Giessen, and A. I. Vakis, 2016, Erratum: “Asperity Interaction and Substrate Deformation in Statistical Summation Models of Contact Between Rough Surfaces” [J. Appl. Mech., 81(4), 041012]. J. Appl. Mech., **83**(8):087001-087001-1.